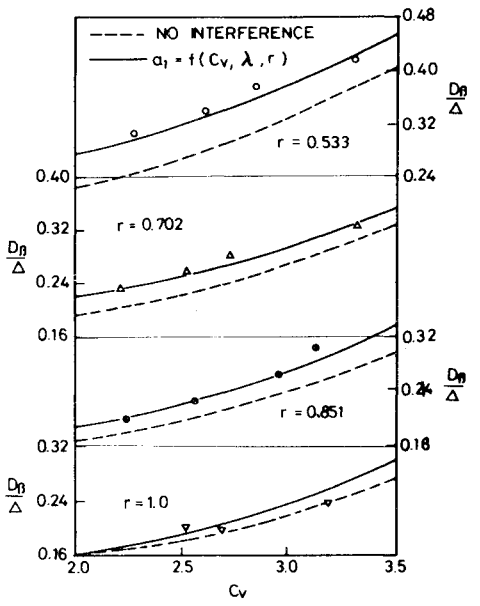

Fig. 2 Comparison with experimental results.[4]

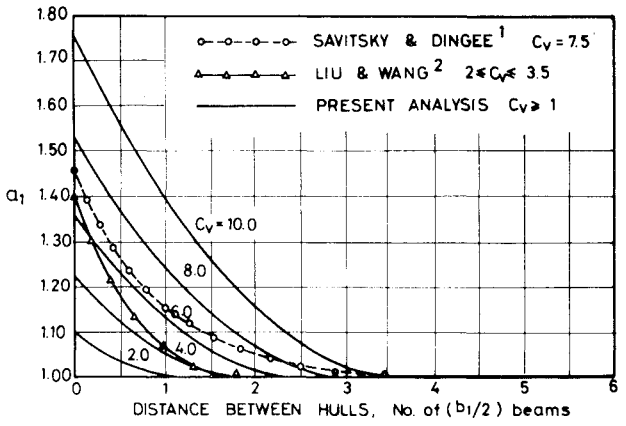

Fig. 3 Interference factor for asymmetric catamaran planing hulls.

The plots of $C_{L0}/\tau^{1.1}$ and $\ell_p/b = C_p\lambda_a$ as a function of C_v and λ_a, with $a_1 = f(C_v, \lambda_a, r)$, are shown in Fig. 1. For a given r, the intersection of C_v vs ℓ_p/b curve gives the corresponding value of $C_{L0}/\tau^{1.1}$, say, m. Therefore at equilibrium running condition, C_{L0} can be expressed in terms of $\tau^{1.1}$ as

$$C_{L0} = m\tau^{1.1} \tag{8}$$

The lift coefficient of the catamaran with deadrise angle is given by Eq. (4) as

$$C_{L\beta} = m\tau^{1.1} - 0.0065\,(m\tau^{1.1})^{0.6} \tag{9}$$

The lift coefficient of the catamaran is also given by

$$C_{L\beta} = \frac{\Delta}{\frac{1}{2}\rho v^2 b_1^2} = \frac{\Delta}{\frac{1}{2}\rho C_v^2 b_1^3 g} \tag{10}$$

Equating (9) and (10), the values of $\tau^{1.1}$ and τ can be obtained by some numerical methods. From this the D_β/Δ ratio can be obtained.

Results and Conclusions

Results of an experimental study of catamaran planing hulls in the towing tanks of the National University of Singapore and National Taiwan University[4] were obtained. They are shown in Fig. 2. It is noted that expressions with interference factors included gave better agreement with the experimental results than expressions with zero interference ($a_1 = 1.0$). Further comparison of the interference factor obtained in this work with that of Savitsky and Dingee[1] and Liu and Wang[2] is shown in Fig. 3. It is observed that the interference factor is a function not only of r, but also of C_v and λ_a. For a fixed r and $1 \leq \lambda_a \leq 4$, the interference effect decreases with increases in separation (i.e., decreases in r). The results also show the applicability of the derived expressions to the hydrodynamics of asymmetric catamaran planing hulls—obtained by considering only the results on single vee-shaped hulls and two flat plates planing parallel to each other.

Acknowledgment

The author gratefully acknowledges the assistance of Professor C.Y. Liu of Universidads Estadual de Campines, Brazil, in the initial stage of this work and would also like to thank G.H.G. Mitchell of the University of Newcastle-Upon-Tyne, England, for providing valuable information on catamaran testing during the writer's attachment at the University of Newcastle-Upon-Tyne between March and June 1980.

References

[1] Savitsky, D. and Dingee, A., "Some Interference Effects Between Two Flat Surfaces Planing Parallel to Each Other at High Speed," *Journal of the Aeronautical Sciences*, Vol. 21, June 1954, pp. 419-420.

[2] Liu, C. Y. and Wang, C. T., "Interference Effect of Catamaran Planing Hulls," *Journal of Hydronautics*, Vol. 13, Jan. 1979, pp. 31-32.

[3] Savitsky, D., "Hydrodynamic Design of Planing Hulls," *Marine Technology*, Vol. 1, Oct. 1964, pp. 71-95.

[4] Wang, C. T., Liu, C. Y., and Guo, C. L., "Effects of the Separation Ratio on the Still Water Resistance of Catamaran Planing Hulls," Institute of Naval Architecture, National Taiwan University Rept. NT-INA-34, May 1975.

[5] Mitchell, G.H.G., "Resistance Experiments on a 1/24th Scale Catamaran Model," University of Newcastle-Upon-Tyne, England, May 1979.

AIAA 81-1900R

Computational Study of the Magnus Effect on Boattailed Shell

W. B. Sturek* and D. C. Mylin†
U.S. Army Ballistic Research Laboratory/ ARRADCOM, Aberdeen Proving Ground, Maryland

Introduction

RECENT papers[1-3] have reported the development and application of the thin-layer parabolized Navier-Stokes computational technique to predict the flow about slender bodies of revolution at supersonic velocities. Reference 3 showed the technique to be a viable computational tool for

Presented as Paper 81-1900 at the AIAA Atmospheric Flight Mechanics Conference, Albuquerque, N. Mex., Aug. 19-21, 1981; submitted Sept. 30, 1981; revision received Jan. 7, 1982. This paper is declared a work of the U.S. Government and therefore is in the public domain.

*Chief, Aerodynamics Research Branch. Associate Fellow AIAA.
†Mathematician, Aerodynamics Research Branch.

Table 1 Summary of boundary conditions for parametric computations

Mach No.	α, deg	PD/V	T_∞, K	p_∞, atm	T_w, K	Freestream Reynolds No., $\times 10^7$/m
2	2	0.19	294	1	239,294,325	4.53
3	2	0.19	294	1	239,294,325	6.80
4	2	0.19	294	1	239,294,325	9.06

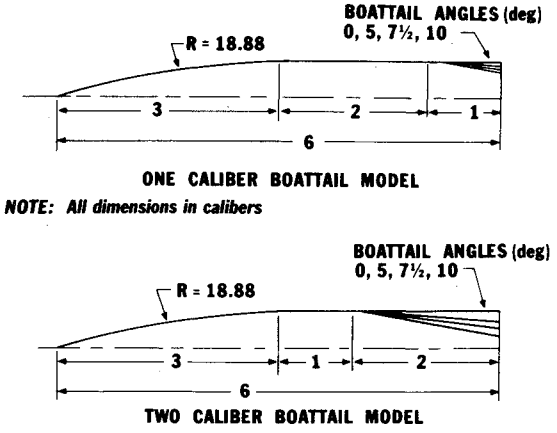

Fig. 1 Model configuration for parametric study.

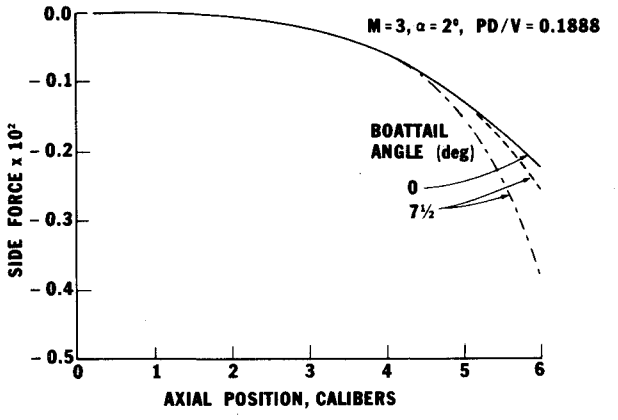

Fig. 2 Magnus force coefficient vs axial position, one and two caliber boattails, $Re = 6.80 \times 10^7$/m.

predicting Magnus effects for a six-caliber slender shell with a one-caliber, 7-deg boattail as verified by comparison to wind-tunnel force measurements. The results of Ref. 3 represent the first successful efforts to compute the Magnus effect for boattailed shell using three-dimensional numerical computational techniques. The objective of this Note is to demonstrate the application of this computational technique to study the flow over spinning shell for a parametric variation of boattail configurations.

Computational Technique

The computational technique solves the steady, thin-layer parabolized Navier-Stokes equations using a numerical algorithm which is an approximately factored, fully implicit, finite difference scheme. The algorithm is conservative and of second-order accuracy in the marching direction. A two-layer algebraic eddy viscosity model[4] is included for the computation of turbulent flows. Details of the parabolized Navier-Stokes assumption and the derivation of the algorithm are included in Ref. 1.

The computations are started from a converged conical solution near the tip of the projectile. The full solution is then

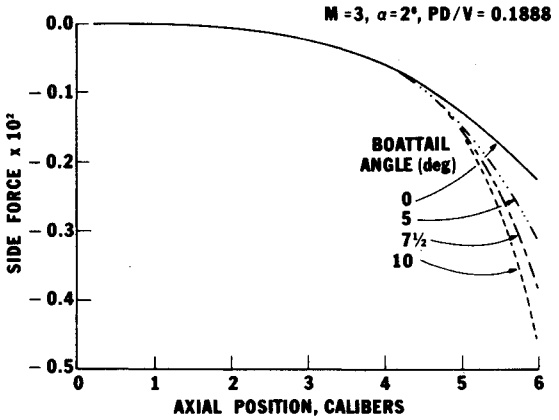

Fig. 3 Magnus force coefficient vs axial position, two caliber boattails, $Re = 6.80 \times 10^7$/m.

obtained by marching over the body in the streamwise (axial) direction. Logarithmic stretching is used to achieve adequate grid resolution of the turbulent viscous layer. The grid generator employs an adaptive capability which insures that adequate resolution of the viscous layer is maintained over the full length of the model. The computational grid consisted of 36 stations about the circumference of the model ($\Delta\phi = 10$ deg) and 50 points between the body and the outer boundary. The streamwise marching stepsize was adjusted to yield 500-800 computational steps for the full length of the shell.

Scope of Computational Effort

A series of computations have been accomplished for a parametric variation of boattail configuration. The geometries are shown in Fig. 1 and include boattail lengths of one and two calibers for boattail angles of 0, 5, 7.5, and 10 deg. This range of boattail length and angle effectively spans the range for practical shell application.

The computations were accomplished for standard atmospheric and wall temperature conditions commonly encountered in projectile firing tests. These conditions are summarized in Table 1.

Magnus Force vs Axial Position

The development of the Magnus force as a function of axial position is shown in Figs. 2 and 3 comparing the effects of boattail length (Fig. 2) and boattail angle (Fig. 3). Figure 2 shows that the length of the boattail strongly affects the magnitude of the Magnus force and that the Magnus force increases with increasing boattail length. Figure 3 shows that the Magnus force increases monotonically for increasing boattail angle for the cases considered here.

Magnus Moment Coefficient vs Mach No.

A parametric comparison for the slope of the Magnus moment aerodynamic coefficient is shown in Fig. 4. The trends indicated are that the Magnus moment coefficient increases with decreasing Mach number, increasing boattail length, and increasing boattail angle. This example illustrates the ability of the computational technique to develop parametric design data which reflect the effects of body configuration and Mach number. These and additional results

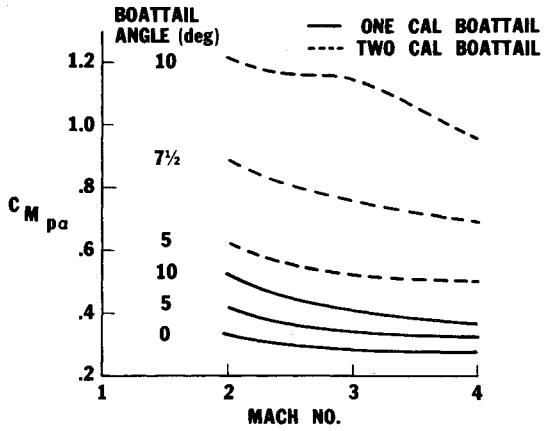

Fig. 4 Slope of Magnus moment coefficient vs Mach number, parametric comparison, $T_\infty = 294$ K, $T_{wall} = 294$ K, c.g. = 3.6 calibers.

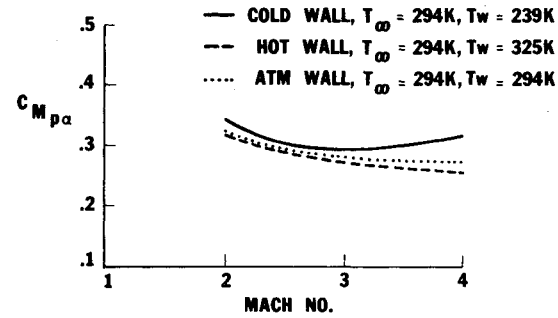

Fig. 5 Slope of Magnus moment coefficient vs Mach number, effect of wall temperature, ogive-cylinder model, c.g. = 3.6 calibers.

will be used to formulate algebraic relationships for use in the development of an interactive design code for the exterior ballistics of shell.

Wall Temperature Effects

In the development and testing of a shell, aerodynamic data are obtained from wind-tunnel tests, aerodynamic range firings, and full range firings. Each of these tests impose different wall temperature boundary conditions for the shell. Additionally, firing tests frequently are carried out in which the shell is temperature conditioned to simulate hot or cold firing conditions. In order to examine the effect of these differing projectile temperature conditions on the aerodynamic behavior, computational results were obtained for hot, cold, standard, and adiabatic wall temperature boundary conditions.

The effect of wall temperature on $C_{M_{p\alpha}}$ is shown in Fig. 5 comparing hot, cold, and atmospheric wall temperatures for a model with a 0-deg boattail angle. The magnitude of $C_{M_{p\alpha}}$ is increased as the wall temperature is decreased. This effect is accentuated at Mach = 4.

Summary

A computational aerodynamics parametric study of the effects of boattail geometry on the Magnus effect for shell has been described in which the thin layer parabolized Navier-Stokes computational technique has been used at supersonic velocities. The computed results show the effects of boattail length and boattail angle for the Magnus effect over a Mach number range $2 \le M \le 4$. Comparisons were also shown which quantize the effects of wall temperature on the Magnus moment coefficient. Parametric results are shown in Ref. 5 for additional pitch and yaw plane aerodynamic coefficients. Comparisons are also shown in Ref. 5 between computed results and wind-tunnel force measurements for Magnus and normal force at angles of attack up to 10 deg. These results indicate that the computational technique gives accurate predictions of the Magnus effect for $\alpha \le 6$ deg.

References

[1] Schiff, L. B. and Steger, J. L., "Numerical Simulation of Steady Supersonic Viscous Flow," *AIAA Journal*, Vol. 18, Dec. 1980, pp. 1421-1430.

[2] Schiff, L. B. and Sturek, W. B., "Numerical Simulation of Steady Supersonic Flow Over an Ogive-Cylinder-Boattail Body," AIAA Paper 80-0066, Jan. 1980.

[3] Sturek, W. B. and Schiff, L. B., "Computations of the Magnus Effect for Slender Bodies in Supersonic Flow," *Proceedings of AIAA Atmospheric Flight Mechanics Conference*, Aug. 1980.

[4] Baldwin, B. S. and Lomax, H., "Thin Layer Approximation and Algebraic Model for Separated Turbulent Flows," AIAA Paper 78-257, 1978.

[5] Sturek, W. B. and Mylin, D. C., "Computational Parametric Study of the Magnus Effect on Boattailed Shell at Supersonic Speeds," *Proceedings of AIAA Atmospheric Flight Mechanics Conference*, Aug. 1981.

AIAA 82-4238

Surface Tension Stability of a Liquid Layer Cooled from Below

Frank G. Collins* and Basil N. Antar†
University of Tennessee Space Institute, Tullahoma, Tennessee

Nomenclature

a	= complex perturbation time constant, $= a_r + ia_i$
A	$= 1 - 1/Pr$
B	= Biot number, $= qd/\kappa$
d	= liquid layer depth
D	= differential operator, $= d/dz$
F,G,H	= functions in Eq. (3)
M	= Marangoni number, $= \sigma\beta d/\mu\kappa$
Pr	= Prandtl number
q	= heat transfer coefficient for free liquid surface
R	$= (F+G)/H$
y	= coordinate parallel to layer surface
z	= coordinate perpendicular to layer lower surface
α	= perturbation wavenumber
β	= temperature gradient of unperturbed liquid layer in z direction
δ	$= (\alpha^2 + ia_i)^{1/2}$
γ	$= (\alpha^2 + ia_i/Pr)^{1/2}$
κ	= liquid thermal diffusivity
σ	= gradient of surface tension with temperature
θ	= perturbation temperature

ONE of the expectations of Spacelab for the processing of new materials is the possibility for the elimination of buoyancy driven convection in the melt. This has revived great interest in obtaining a more complete understanding of the Benard convection problem. In Spacelab the dominant force imposed on a melt will be the surface tension force.

Received Dec. 15, 1981.

*Professor, Aerospace Engineering. Member AIAA.
†Associate Professor, Engineering Science and Mechanics.